HHS Public Access

Author manuscript

*Nano Lett*. Author manuscript; available in PMC 2020 April 10.

Published in final edited form as:

*Nano Lett*. 2019 June 12; 19(6): 4017–4022. doi:10.1021/acs.nanolett.9b01254.

# Electronic Decay Length in a Protein Molecule

**Bintian Zhang**[1], **Stuart Lindsay**[1,2,3]

[1]Biodesign Institute, Arizona State University, Tempe, AZ 85287

[2]Department of Physics, Arizona State University, Tempe, AZ 85287

[3]School of Molecular Sciences, Arizona State University, Tempe, AZ 85287

## Abstract

Antibodies have two identical binding domains, and can therefore form a well-defined conducting bridge by binding a pair of electrodes functionalized with an epitope. The conductance measured between these two fixed points on the antibody does not change with the size of the electrode gap. A second conduction path is via one specific attachment to an epitope and a second non-specific attachment to the surface of the antibody. In this case, the conductance does change with gap size, yielding an estimated electronic decay length > 6nm, long enough that it is not possible to distinguish between an exponential or a hyperbolic distance dependence. This decay length is substantially greater than that measured for hopping transport in an organic molecular wire.

## Graphical Abstract

*Corresponding Author: Stuart Lindsay, Stuart.Lindsay@asu.edu.

Author Contributions

The manuscript was written through contributions of both authors. Both authors have given approval to the final version of the manuscript.

**Supporting Information**: Methods, Figures S1, S2 conductance distributions. Tables S1–S8 fitting parameters.

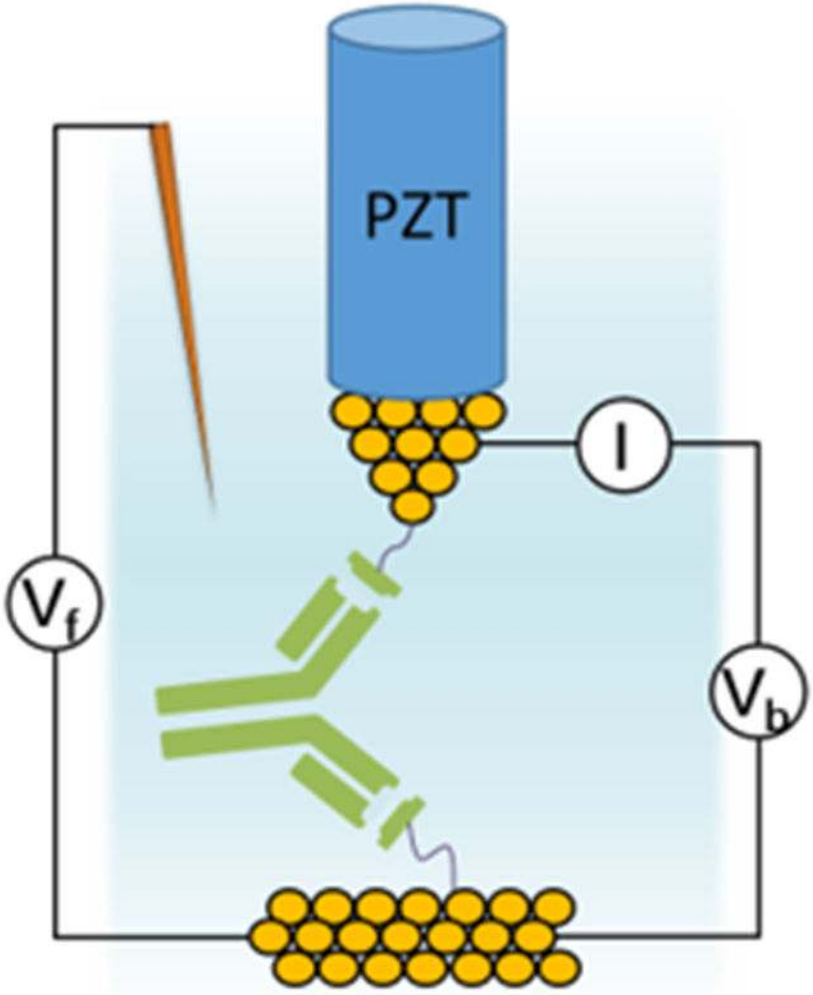


**Keywords**

Molecular electronics; bioelectronics; protein conductance; electronic decay length

Proteins are remarkably versatile molecular machines, capable of molecular recognition, highly selective catalysis, directional energy transfer, directed polymer synthesis and many other functions, so integration of proteins into bioelectronic devices has been a long sought-after goal[1]. Electrical measurements on peptides[2–6] find values for the decay constant, β, in the range of 5 to 10 $nm^{-1}$. The transport is assumed to be tunneling, where the distance dependence of conductance is given by $G(z) = G_0 \exp(-\beta z)$, with $G_0$ being the quantum of conductance for a quantum point contact. In contrast, measurements on intact proteins suggest that they transport electrons more efficiently than even conjugated molecules[7] with β values of 2 $nm^{-1}$ or less. Petrov et al.[8] predict a transition to a weak distance dependence for longer peptides when activated hopping becomes the dominant transport mechanism. This transition has been observed in optical studies,[9,10] but has not been observed in conductance experiments on the same peptides.[5] Clearly transport mechanisms can differ: in optical experiments, carrier injection occurs via a ~2eV barrier[9] whereas charge injection at

a metal electrode can be nearly barrier-free.[11] A second complication arises from the different electrical measurement techniques used for peptides and proteins: It is straightforward to make measurements on a series of small peptides of different lengths in order to deduce a value for β.[2] In the case of intact proteins, β was inferred from measurements on proteins of different sizes, and on multilayer stacks of proteins.[7] The distance dependence of conductance can be measured directly for long filamentous protein aggregates, and the pili of *Geobacter sulfurreducans* have been shown to have conductivities that approach those of metallic nanowires.[12, 13] For proteins that do not aggregate into long wires, a key challenge lies in the way that contacts are made between electrodes and a protein molecule.[11] Among the findings of our recent work[11] are: (a) The specific ligand that a protein has evolved to bind forms a reproducible high conductance (nS over nm distances) contact. (b) One such specific contact is adequate for obtaining a significant conductance, even if the second contact is via a weak interaction. (c) Non-covalent binding to a ligand attached to an electrode gives significantly higher conductance than direct attachment via covalent modification of surface residues. (d) Attachment via two ligand binding sites on a multivalent protein increases the conductance approximately ten-fold relative to one specific and one weak, non-specific, contact. (e) The measured conductance via two specific contacts does not change with the gap distance between the electrodes. In a key experiment, we used antibodies to show that the conduction path passes through the proteins and not through space. When antibodies bind epitope-functionalized electrodes, their conductance distributions have two peaks, one (Peak 1) at around 0.2 nS and a second (Peak 2) at around 2nS. In contrast, proteins tethered by only one specific contact showed only a single peak (Peak 1) in the conductance distribution. We associated Peak 1 with one specific contact at the ligand binding site and a second non-specific contact at some other point on the protein. In the antibodies, we interpreted Peak 1 the same way (as one specific contact and one non-specific contact) and we attributed Peak 2 to conduction via specific bonds at the two antigen binding sites (i.e., Fv domains, see Figure 2e). This interpretation was tested by (i) using one electrode functionalized with an epitope and a second electrode functionalized with mercaptoethanol (to make it hydrophilic so that it could contact surface hydrophilic residues) and (ii) Using two epitope-functionalized electrodes with a Fab fragment from the antibody (consisting of just one arm of the antibody - Figure 2e). Both experiments produced just Peak 1 (at ~0.2nS) in the conductance distributions, showing that Peak 2 is a consequence of two specific binding events that bridge the two electrodes. In that previous work, we stated that the peaks in the conductance distributions appeared to be independent of the size of the electrode gap contacting the proteins, but careful inspection of the data shows that this is not entirely the case. Here, we exploit the variable nature of the non-specific contact (NS) to examine the gap distance dependence of protein conductance more closely. We have also measured the distance dependence using one specific contact (S - epitope to antibody) and one small-molecule (mercaptoethanol - MCE) NS contact, an arrangement that shows the distance dependence more clearly. We have measured the conductance distributions of an anti-Ebola IgG out to a gap distance of ~ 6.5 nm, and have made similar measurements on a Fab fragment prepared from the same antibody out to ~ 3.5 nm, beyond which point the gap is larger than the height of the Fab fragment. The IgG yields data out to 6.5 nm which is greater than the 6nm length of the Fab fragment. Thus the data obtained on the Fab fragment must correspond to a shorter path through the protein than the

data obtained from the intact antibody. This, then, provides a method for estimating the electronic decay length in a given protein, without the complications of comparing different proteins or of making measurements on multilayers. In the data we report here, we find a small, but systematic, decrease in conductance with distance for Peak 1 in data from both IgG and IgE antibodies, suggesting that the second, non-specific contact is, to some extent, a 'sliding' contact. This change is clearest (i.e., best fit to an exponential) when one specific contact is made via an epitope with the second, non-specific contact made via mercaptoethanol, a small molecule that renders the electrode capable of hydrogen bonding to surface residues. In contrast the values of conductance for Peak 2 show no significant change of conductance with gap size, consistent with the interpretation that Peak 2 arises from two contact points fixed on the protein. In what follows we refer to electron transport for convenience. We have no experimental data on the sign of the charge carriers, and indeed, the proximity of bands associated with oxidizable amino acid residues to the metal Fermi Energy[11] suggests that hole transport is more likely.

Our measurements were made using an electrochemical scanning tunneling microscope (Pico STM, Agilent) with insulated palladium (Pd) probes[14] and a Pd substrate, both held under potential control using a salt-bridged reference electrode (Fig. 1a). We chose proteins with no electrochemical activity in the range of potentials studied (thus avoiding Faradaic currents). In the present study we used two antibodies, an IgG raised against the Ebola virus and an IgE raised against dinitrophenol (DNP). In both cases, the epitope was diluted 20:1 with mercaptoethanol when functionalizing the substrate to reduce the density of antibody binding sites, so as to increase the probability that one of the two antibody binding domains remained unattached and available for binding to the epitope-functionalized probe. This increased the frequency of specific binding events dramatically. For the anti-Ebola IgG, the epitope was a peptide with the sequence CHNTPVYKLDISEATQV where the cysteine residue (C) provides the thiol for attachment to the Pd electrodes. For the IgE, we synthesized N,N'-bis(2,4-dinitrophenyl)cystamine in house, reducing it to a thiolated dinitrophenol (DNP) for attachment to the electrodes.[11] We also carried out measurements with the substrate modified with peptide epitope and the probe modified with mercaptoethanol. Current-voltage (IV) characteristics were measured using a constant fixed gap (no servo control). The gap remained constant to within about 0.1nm over ~ 1 minute, and the bias was swept between −0.2 and +0.2V and back again at a rate of 1V/s. It is important to emphasize that the gap remained constant during measurement - no attempt was made to fish for proteins or to push or pull them. Thus the trapped proteins that yielded signals were molecules that bound across the gap in equilibrium, or near equilibrium conformations. After 1 minute, the gap was returned to the set-point value (labeled $Z_0$ in the Figures here), the current recorded to check that there had been no significant drift, and the servo re-engaged. The cycle was then repeated to obtain further IV sweeps. 80% of these IV sweeps were perfectly reproducible (up-sweep vs. down sweep) and were completely linear, yielding a single conductance value for each scan (Fig. 1b). Some 1000 sweeps were acquired in each run at each gap value. Full details of the experimental methods, controls and materials are given in an earlier publication and its accompanying online supplementary material[11] as well as the Supporting Information for the present letter. In the present work, we have extended our measurements to study the distance dependence of the conductance

distributions measured for the full anti-Ebola IgG antibody, and for a Fab fragment derived from it. The Fab consists of one constant and one variable domain of each of the light and heavy chains of the parent antibody. The full antibody spans about 15 nm between the two binding sites[15] (RSC PDB structure 1IGT) and the Fab is about 6 nm in length (RSC PDB structure 1YUH). Both structures are about 4 nm high (if lying flat on the substrate). The structure of the full antibody viewed in the plane of its largest dimension is shown in Figure 2e. The three domains (2 Fabs and the stem) are coupled via flexible peptide sequences, so are likely to fluctuate from the crystal structure in solution. The substrate has been treated so as to be hydrophilic, so and an antibody trapped between the probe and substrate is likely to be confined in the semi-flat conformations shown in Figures 2 c and d (illustrations are to scale using the structures given in the RSC PDB). Figure 2 shows representative conductance distributions for the anti-Ebola IgG (Fig. 2a) and the Fab obtained from it (Fig. 2b). The maroon dots are from the down-sweeps and the dark yellow dots are from the up sweeps. These distributions capture all the types of contacts that occur in repeated experiments (~1000x per distribution), so while contacts are highly variable, the distributions themselves are not, and we use the fitted peak values as characteristic of the most probable contact configurations in the gaps. As reported earlier for other proteins[11], the peaks values of the conductance distributions do not change much with gap size, but the frequency with which the proteins are contacted decreases, presumably because the available area of the probe over which contact can be made decreases with the height of the probe above the substrate (~1000 sweeps were acquired in all cases, but fewer of them gave a response at the larger gaps).

As discussed earlier, Peak 2 (around 2nS) is generated by contact events with two specific bonds, illustrated by the red fuzzy circles on Fig. 2d. Peak 1 (Fig. 2c) is a consequence of one specific bond (red fuzzy circle) and one non-specific bond (blue fuzzy circle). $Z_0$ is determined by the initial gap set point (4pA at −0.2V). This 20 pS conductance corresponds to a gap of about 2.5 nm (as determined using a 'chemical ruler'[16] ) so that the largest gap at which data were obtained from the Fab was about 3.5 nm. This corresponds to the shortest dimension of the Fab (it is about 6 nm long), suggesting that the Fab lies flat on the substrate and is unlikely to fluctuate into a vertical geometry. In the case of the anti-Ebola IgG, the largest gap was about 6.5 nm. This is much less than the head to head distance of about 15 nm, again suggesting that the full IgG molecule is unlikely to fluctuate into a vertical position. Plots of the peak positions are shown in Figure 3 (a: Peak 1, b: Peak 2). These peak positions are obtained from the conductance distributions in Figures 2, and Supporting Information, Figures S1 and S2. Error bars are the uncertainties in the Gaussian fits to the distributions of the logarithm of G (lines in Figure 2). As reported earlier, [11] having the epitope on only one electrode (MCE second contact) results in only a single peak in the conductance distribution (Figure S2). Here, natural logarithms are used so that the slope yields the inverse electronic decay length. Green symbols are for the Fab, blue for the IgG and red are for the anti-DNP IgE. Black squares are for the IgG attached by one peptide epitope and probed with MCE. A distance dependence is reasonably clear in the cases where small molecule contacts were used (black and red data points) but not so obvious where two peptide contacts were used (blue and green data points).

For this reason the measurements with peptide contacts were repeated three times (Supporting Information, Figure S1), and the data points at each gap value averaged to give the orange data points. We attribute this greater variability in the case of two peptide contacts to the relatively large size of the peptide (17 aa corresponds to about a 1 nm radius of gyration). In the case of the specific contact, it is folded into the binding pocket, but in the case of a non-specific contact it could make contacts that are as remote as its extended length (~4nm). Fitted slopes for all three types of contact are shown in Table 1. A key observation is that the Peak 1 conductances measured for the Fab at a gap of 2.5 nm are significantly higher than the Peak 1 conductances measured for the IgG at 6.5 nm (Fig. 3a). In contrast, there is no significant difference between the conductances measured at 3.5 nm and 6.5 nm for Peak 2 (Fig. 3b) where the conduction path remains constant. The fits to Peak 2 yield $\ln(G) = 1.0 \pm 0.08 - (0.03 \pm 0.02)Z$, $R^2$=0.4 (IgE) These fits yield a contact resistance of about 350MΩ. The second, non-specific contact that yields Peak 1 must depend on the chemical nature of the antibody (or Fab) surface, but nonetheless, there is a significant systematic downward trend with distance for both antibodies and the Fab.

All three types of contact yield a statistically significant distance dependence with $0.1<\beta<0.15$. The result is most convincing in the case of the IgG molecule attached to the substrate by a peptide epitope and probed with an MCE contact ($R^2$=0.96). The data are more variable with a small epitope (DNP) on both electrodes, presumably because the antibody can attach specifically to either probe or substrate. For the case of a peptide epitope on both electrodes, the spread is larger ($R^2$ = 0.43 without averaging of the 3 runs, 0.91 when averaged data are used), reflecting the variability of the non-specific contact made with a peptide. Using the most reliable value of $\beta=0.16\pm0.02$ $nm^{-1}$ gives a decay length, $\lambda = \beta^{-1}$ of 6.2 nm. Since this is nearly equal to the size of the largest gap used, it is not possible to distinguish between an exponential and a 1/Z decay: A fit to $G(z) = 1/(R_0 + Az)$ has an R value of 0.65 (dashed line on Fig. 3a).

The results for Peak 1 and Peak 2 were obtained from the same experimental data sets, lending credence to the observed distance dependence of Peak 1. Our value for the electronic decay length assumes that changes in the electrode gap correspond to changes in the path length through the protein. This is unlikely because of the irregular contours of the antibody surface and the existence of discrete binding sites. Nonetheless, the actual path length cannot be *less* that the actual gap, so the derived values of β must be an upper limit. In other words, λ is *at least* ~ 6 nm. The illustrations in Figure 2c show geometries for the case of the S-NS in which the shortest direct path is taken, so that the gap size and the path length do not differ much. The high resistance of the non-specific contact rules out the possibility of arm-to-arm contacts across the 15 nm dimension of the antibody: Assuming an overall resistance, $R$, given by $R = R_0\exp(\beta Z)$, the 2.2 GΩ contact resistance yields an overall resistance of 21GΩ, or a conductance of 0.04 nS, considerably smaller than the observed 0.2 nS. Applying the same calculation to the S-S contacts ($R_0$ = 370MΩ) yields a conductance of 0.3 nS over 15 nm, not an unreasonable value, although this approach is questionable because the peak 2 data most likely reflect a combination of contact resistance and a constant internal resistance. Another way to look at this is to calculate what contact resistance would be consistent with an overall resistance of 370MΩ, β=0.16 and Z= 15 nm. The value is 40MΩ, well within the range of contact resistances measured for short peptides.[2,4,6,5]

The MCE contact has a significantly lower contact resistance (1.35 GΩ) but yields a slope that is within about a standard deviation of that yielded by the other types of contact. Thus a very different contact (in terms of contact resistance) yields about the same slope. This lends support to the interpretation that the gap size is quite close to the actual path length through the protein for the case of the S-NS contacts.

An electronic decay length of 6 nm is a significant fraction of the mean-free path of electrons in the best metallic conductors at room temperature.[17] This is a surprising result, as proteins are often viewed as insulating materials. Nonetheless it is consistent with the remarkably small decay of current density with protein size, as reviewed by Amdursky et al.[7]

In order to compare the present results with previous measurements on peptides, we have extracted data in the form of natural log of resistance vs. distance (Fig. 3c) from the publications listed in the caption. The peptide measurements tie in with the Peak 1 data for the IgG and IgE quite well, in as much as they are consistent with the high contact resistance we observe (Table 1). They suggest a model in which the injection of carriers is limited by tunneling decay in the peptide sequence closest to the electrode, while the long decay length in the bulk protein reflects the long range hopping proposed by Petrov et al.[8] We have used the language of resistances for convenience, but the exponential dependence on distance multiplied by the contact resistance implies two sequential processes: tunneling into the protein, via the surface peptide contact, followed by hopping transport within the protein. Clearly, this model requires further experimental tests.

A transition from tunneling to hopping conductance as a function of length was first reported for a molecular wire by Choi et al.[18] with results that look similar to Fig 3c, except for the value of β in the hopping regime (0.9 $nm^{-1}$ for an oligophenylineamide wire, 0.1 $nm^{-1}$ for these proteins). 0.9 $nm^{-1}$ not too different from the 1.8 $nm^{-1}$ measured optically for a long peptide in the hopping regime.[10] Why does the protein interior appear to be so much better as a hopping conductor than either an aromatic molecular wire or a long peptide? Matyushov[19] has carried out an analysis of solvent-induced fluctuations in the interior of a protein, finding that the placement of charges and dipoles on the hydrophilic exterior of the protein is, in many proteins, optimized such that the resulting fluctuations lower barriers to tunneling. Further, rapid transport leads to a significant reduction in trapping energy. Isolated peptides and organic molecular wires lack this dielectric shell. It may be that the effectiveness of a specific ligand as a contact lies in its ability to inject electrons or holes through this external shell.

Fig. 3c also shows a point for Peak 2 for the IgG molecule (purple triangle) and for streptavidin (red star) connected to electrodes via a thiolated biotin molecule[11] (with both data points placed at the largest gap distance measured). They illustrate how the contact resistance falls with two specific contacts (IgG) and two even stronger specific contacts (biotin-streptavidin). Indeed, the resistance of the biotin-streptavidin-biotin complex in a 3.5 nm junction is a remarkably low 150MΩ, illustrating what effective molecular wires proteins can be. Further experimental and theoretical work is needed to understand this electrical

conductivity, including exploration of novel quantum aspects of protein electronic structure.[20]

## Supplementary Material

Refer to Web version on PubMed Central for supplementary material.

## Acknowledgements

We are grateful to David Cahen, David Beratan and Dmitry Matyushov for useful discussions. The anti-Ebola IgG and corresponding Fab fragment were prepared by Huafang Lai and Qiang Chen. Ben Miller synthesized the N,N'-bis(2,4-dinitrophenyl)cystamine.

Funding Sources

This work was funded in part by the NHGRI (grant number R01 HG009180), Recognition AnalytiX LLC and the Edward and Nadine Carson Endowment.

## References

1. Bostick CD; Mukhopadhyay S; Pecht I; Sheves M; Cahen D; Lederman D Reports on Progress in Physics 2018, 81, 026601. [PubMed: 29303117]
2. Xiao X; Xu B; Tao N Journal of the American Chemical Society 2004, 126, (17), 5370–1. [PubMed: 15113203]
3. Sepunaru L; Refaely-Abramson S; Lovrincic R; Gavrilov Y; Agrawal P; Levy Y; Kronik L; Pecht I; Sheves M; Cahen D Journal of the American Chemical Society 2015, 137, (30), 9617–26. [PubMed: 26149234]
4. Brisendine JM; Refaely-Abramson S; Liu Z-F; Cui J; Ng F; Neaton JB; Koder RL; Venkataraman L The journal of physical chemistry letters 2018, 9, (4), 763–767. [PubMed: 29376375]
5. Sek S; Misicka A; Swiatek K; Maicka E J Phys Chem B 2006, 110, (39), 19671–7. [PubMed: 17004836]
6. Juhaniewicz J; Sek S Bioelectrochemistry 2012, 87, 21–7. [PubMed: 22197550]
7. Amdursky Nadav; Marchak Debora; Sepunaru Lior; Pecht Israel; Sheves Mordechai; Cahen D. Advanced Materials 2014, 26, 7142–7161. [PubMed: 25256438]
8. Petrov EG; Shevchenko YV; Teslenko VI J. Chem. Phys 2001, 115, 7107–7122.
9. Aubert C; Vos MH; Mathis P; Eker AP; Brettel K Nature 2000, 405, (6786), 586–90. [PubMed: 10850720]
10. Malak RA; Gao Z; Wishart JF; Isied SS Journal of the American Chemical Society 2004, 126, (43), 13888–9. [PubMed: 15506726]
11. Zhang B; Song W; Pang P; Lai H; Chen Q; Zhang P; Lindsay S Proc Natl Acad Sci U S A 2019, 10.1073/pnas.1819674116.
12. Adhikari RY; Malvankar NS; Tuominen MT; Lovley DR RSC Advances 2016, 6, 8354–8357.
13. Malvankar NS; Vargas M; Nevin KP; Franks AE; Leang C; Kim BC; Inoue K; Mester T; Covalla SF; Johnson JP; Rotello VM; Tuominen MT; Lovley DR Nat Nanotechnol 2011, 6, (9), 573–9. [PubMed: 21822253]
14. Tuchband M; He J; Huang S; Lindsay S Rev Sci Instrum 2012, 83, (1), 015102. [PubMed: 22299981]
15. Tan YH; Liu M; Nolting B; Go JG; Gervay-Hague J; Liu GY ACS Nano 2008, 2, (11), 2374–84. [PubMed: 19206405]
16. Chang S; He J; Zhang P; Gyarfas B; Lindsay S Journal of the American Chemical Society 2011, 133, (36), 14267–9. [PubMed: 21838292]
17. Gall DJ Appl. Phys 2016, 119, 085101–085106.
18. Ho Choi S; Kim B; Frisbie CD Science (New York, N.Y.) 2008, 320, (5882), 1482–6.

19. Matyushov DV J Chem Phys 2013, 139, (2), 025102. [PubMed: 23862967]
20. Vattay G.a. ; Salahub D; Csabai I. a.; Nassimi A; Kaufmann SA. Journal of Physics: Conference Series 2015, 626, 012023.

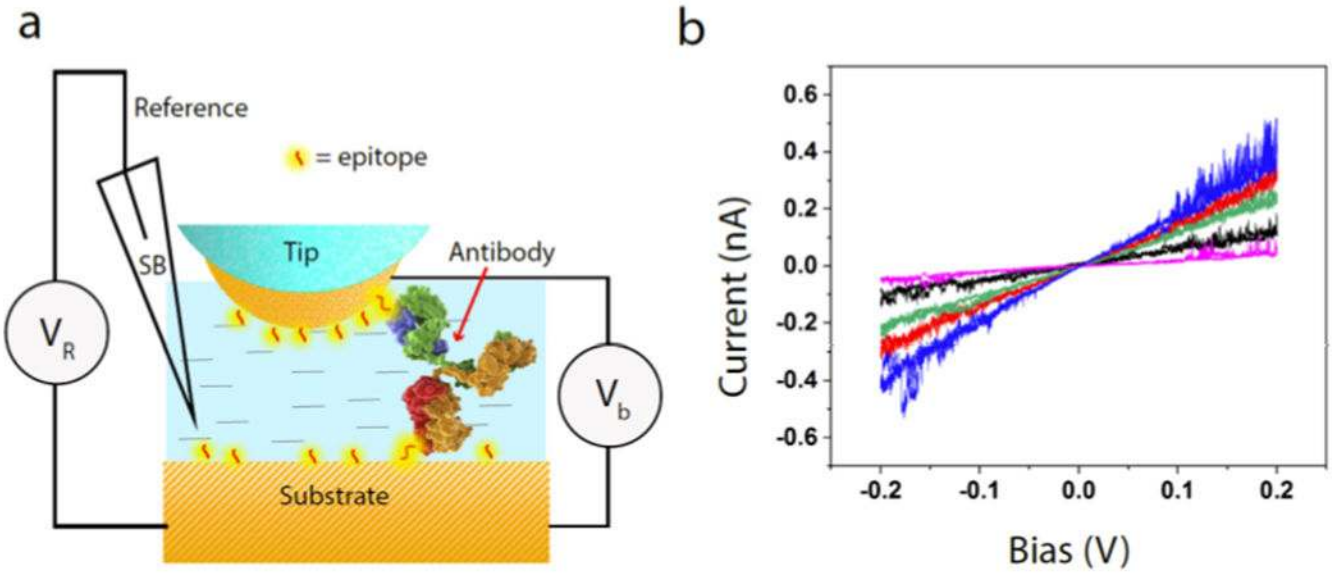


**Figure 1:**

STM measurements of single-molecule conductance (a) A partially insulated STM probe is immersed in electrolyte (1 mM phosphate buffer, pH 7.4) and functionalized with thiolated epitope molecules, as is the substrate. The surface potential of the substrate ($V_R$) is chosen so that the substrate and tip (potential $V_R+V_B$) generate no Faradaic current (SB is a salt-bridged reference electrode). When the gap is small enough, an antibody can bind between tip and substrate (see Figure 2 for likely geometries). (b) A sample of IV curves obtained from the anti-Ebola IgG. On each trace, up-sweep and down-sweep are superimposed, showing the reproducibility. Above 100mV, bias induced fluctuations of the contacts generate telegraph noise.

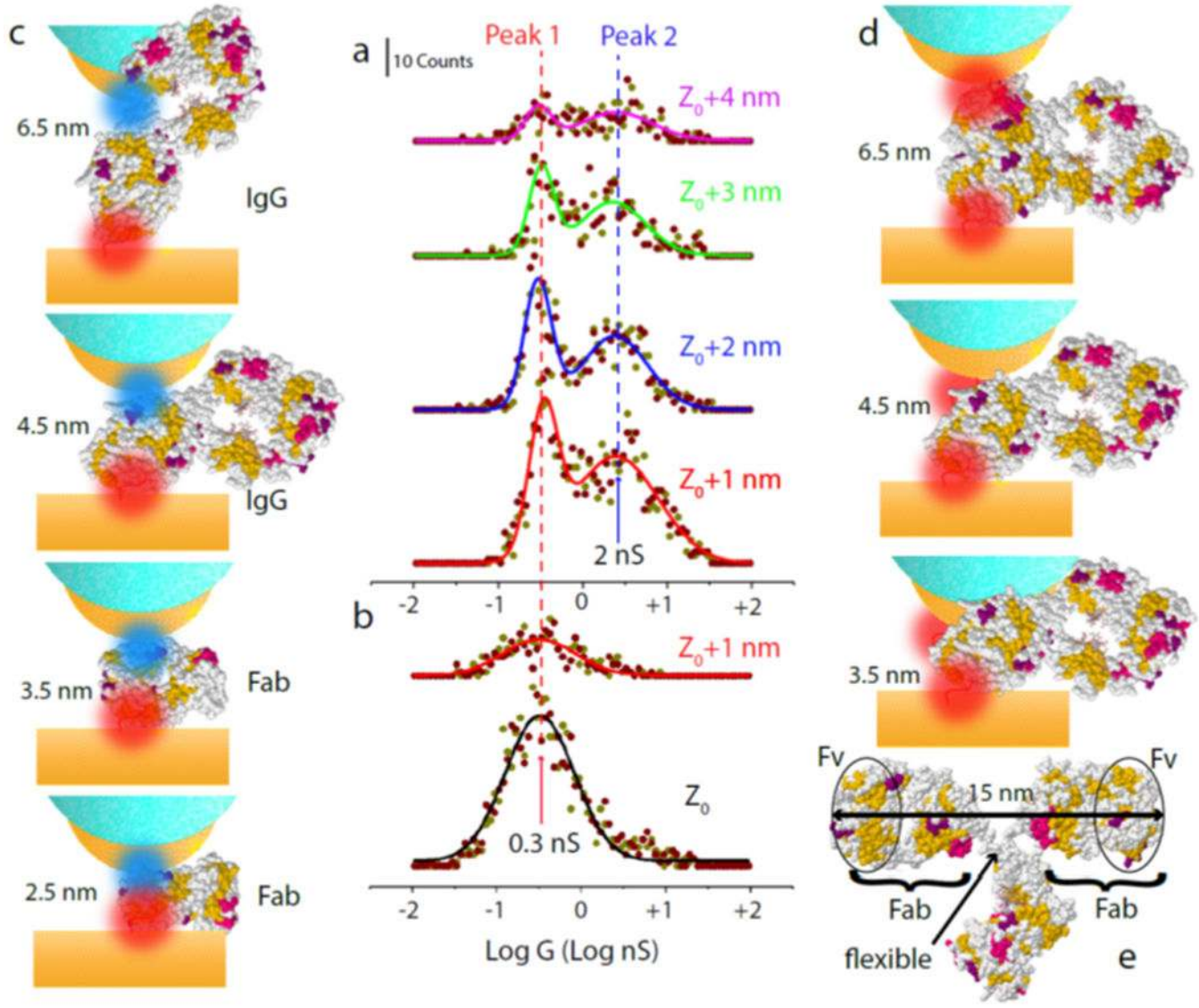


**Figure 2:**

Distributions of the logarithm (base 10) of the conductances measured from current-voltage curves recorded on individual IgG antibodies (a) and a Fab fragment obtained from the same antibody (b). Distributions are shown for gap increments as shown from the original set-point gap, $Z_0$ (about 2.5 nm). All distributions have a peak corresponding to 0.2 nS (Peak 1), while the intact antibody distributions have a second peak at ~ 2nS (Peak 2). Peak 1 corresponds to one attachment via specific bonding to an epitope-functionalized electrode and a second attachment via a non-specific attachment at some point on the surface of the protein (S-NS). Peak 2 corresponds to the fixed path between the two binding heads (S-S). Possible geometries for S-NS (S=red, NS=blue) contacts are illustrated to scale in (c) for various gaps. S-S contacts are illustrated in (d). The dimension of the IgG lying flat are illustrated in (e). The simple correlation between the number of peaks and the number of specific contacts indicates that contacts to more than one molecule are infrequent enough so

that additional high conductance peaks are not observed at multiples of the two fundamental values. Solid lines are Gaussian fits to the distributions.

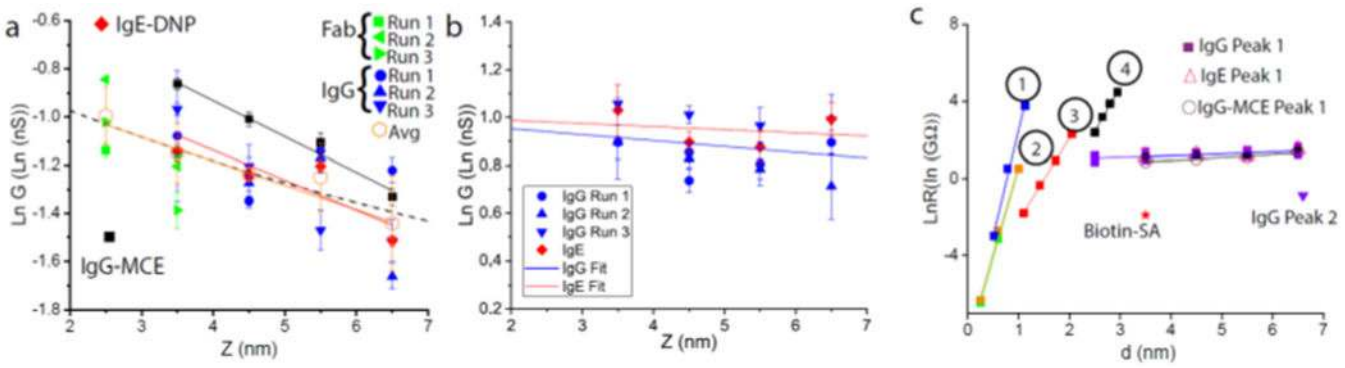


**Figure 3:**

Plots of the natural logarithm (base e) of the conductance peaks obtained from Gaussian fits to the measured distributions for Peak 1 (a) and Peak 2 (b). Green symbols are for the Fab fragment, blue for the IgG with peptide epitopes on both electrodes, black is for the IgG with peptide epitope on one electrode and mercaptoethanol (MCE) on the other, and red is for the IgE antibody binding DNP on the electrodes (conductance distributions for the IgE molecule are shown in reference [11]). Data from three different experimental runs are shown for the Fab and IgG by different symbols, where the error bars show the uncertainty in the Gaussian fits to the distributions of $Log_{10}$ (G). The three runs for the Fab and IgG were averaged (orange data points) before fitting (orange line). The red line is a fit to the IgE data points, and the black line is a fit to the peptide-MCE combination data. The IgG data are fitted almost as well by a 1/Z dependence, shown by the dashed line. (c) Summary of ln(R) (units ln(GΩ)) for the proteins with three different contacts (purple squares, circles and triangles) and 5 different peptides ("2" shows overlapped data for two sequences) of various lengths: "1" is ref. [2], "2" is ref. [4], "3" is ref.[6] and "4" is ref [5].

**Table 1:**

Fits to the gap-distance dependence of peak 1 (Figure 3a).

| | **IgG-Epitopes** | **IgE-DNP** | **IgG-MCE** |
|---|---|---|---|
| Contacts | CHNTPVYKLDISEATQV | HSCH2CH2-dinitrophenol (DNP) | 1) CHNTPVYKLDISEATQV<br>2) Mercaptoethanol (MCE) |
| Slope, β ($nm^{-1}$) | 0.100±0.018 | 0.109±0.047 | 0.156±0.021 |
| Intercept, GΩ | 2.18±0.17 | 2.19±0.45 | 1.35±0.16 |
| $R^2$ | 0.91 | 0.73 | 0.96 |